Early Science with the Large Millimeter Telescope: discovery of the ^{12}CO(1–0) emission line in the ring galaxy VIIZw466

O. Ivy Wong,[1,2]★ O. Vega,[3] D. Sánchez-Argüelles,[3] G. Narayanan,[4] W. F. Wall,[3] M. A. Zwaan,[5] D. Rosa González,[3] M. Zeballos,[3] K. Bekki,[1] Y. D. Mayya,[3] A. Montaña[3,6] and A. Chung[7]

[1]*International Centre for Radio Astronomy Research, University of Western Australia M468, 35 Stirling Highway, Crawley, WA 6009, Australia*
[2]*ARC Centre of Excellence for All-Sky Astrophysics (CAASTRO), Australia*
[3]*Instituto Nacional de Astrofísica, Optica y Electrónica, Luis Enrique Erro 1, Tonantzintla, Puebla C.P. 72840, México*
[4]*Department of Astronomy, University of Massachusetts, Amherst, MA 01003, USA*
[5]*European Southern Observatory, Karl-Schwarzschild-Str. 2, D-85748 Garching bei München, Germany*
[6]*Consejo Nacional de Ciencia y Tecnología, Av. Insurgentes Sur 1582, Col. Crédito Constructor, Del. Benito Juárez, C.P. 03940 México, D.F., México, Mexico*
[7]*Department of Astronomy & Yonsei University Observatory, Yonsei University, 50 Yonsei-ro, Seodaemun-gu, Seoul 120-749, Korea*

ABSTRACT

We report an early science discovery of the ^{12}CO(1–0) emission line in the collisional ring galaxy VII Zw466, using the Redshift Search Receiver instrument on the Large Millimeter Telescope Alfonso Serrano. The apparent molecular-to-atomic gas ratio either places the interstellar medium (ISM) of VII Zw466 in the H I-dominated regime or implies a large quantity of CO-dark molecular gas, given its high star formation rate. The molecular gas densities and star formation rate densities of VII Zw466 are consistent with the standard Kennicutt–Schmidt star formation law even though we find this galaxy to be H$_2$-deficient. The choice of CO-to-H$_2$ conversion factors cannot explain the apparent H$_2$ deficiency in its entirety. Hence, we find that the collisional ring galaxy, VII Zw466, is either largely deficient in both H$_2$ and H I or contains a large mass of CO-dark gas. A low molecular gas fraction could be due to the enhancement of feedback processes from previous episodes of star formation as a result of the star-forming ISM being confined to the ring. We conclude that collisional ring galaxy formation is an extreme form of galaxy interaction that triggers a strong galactic-wide burst of star formation that may provide immediate negative feedback towards subsequent episodes of star formation – resulting in a short-lived star formation history or, at least, the appearance of a molecular gas deficit.

Key words: ISM: molecules – galaxies: evolution – galaxies: formation – galaxies: individual: VII Zw466.

1 INTRODUCTION

Drop-through or collisional ring galaxies are unique astrophysical objects in that the physical mechanism that drives the ring formation – that of expanding density waves – are very well-understood. The process of star formation plays a vital role in the evolution of galaxies. In collisional ring galaxies, the star formation within the ring is a result of the interaction-triggered density waves that compress the cold gas in the galaxy's interstellar medium (ISM; e.g. Lynds & Toomre 1976; Wong et al. 2006).

Similar to the prototypical collisional ring galaxy, the Cartwheel galaxy (A0035−33; e.g. Appleton, Charmandaris & Struck 1996; Higdon et al. 2015), VII Zw466 is a collisional ring galaxy in a compact galaxy group with two other massive companion galaxies (see Fig. 1). However, this is where the similarity ends. VII Zw466 has been classified as an empty ring (RE) galaxy and the result of an off-centre collision (Fiacconi et al. 2012; Mapelli & Mayer 2012), while the Cartwheel is likely a product of a nuclear collision (Appleton & Marston 1997). Also, observations have found VII Zw466 to consist of an ISM with solar metallicities (Bransford et al. 1998). Hence, the combination of the ring formation process and the metallicity suggests that VII Zw466 is more similar to AM0644−741 (Higdon, Higdon & Rand 2011) and NGC 922 (Wong et al. 2006). An H I bridge connects VII Zw466 and its southern companion, G2 (see
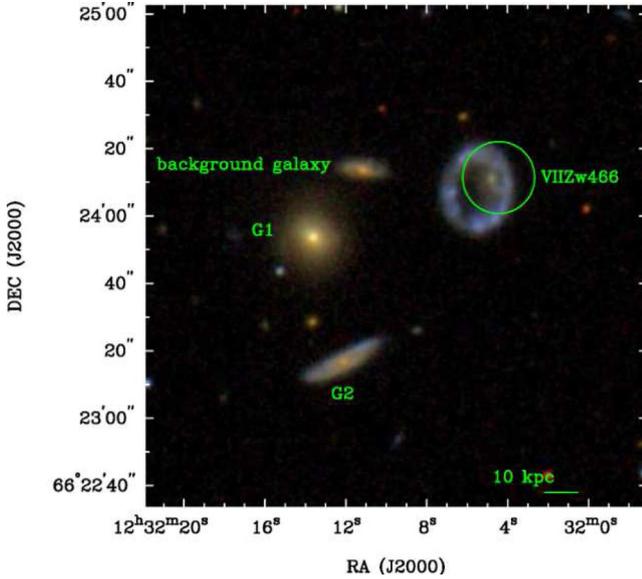
★ E-mail: ivy.wong@uwa.edu.au

Figure 1. Three-colour SDSS DR12 (Alam et al. 2015) map of VII Zw466 and its two neighbouring galaxies, labelled 'G1' and 'G2'. Blue: *g* band; green: *r* band; and red: *i* band. The green circle marks a representative 20-arcsec beam centred on the LMT pointing described in this paper. The southern companion galaxy G2 is thought to be the intruder galaxy that triggered the formation of the star-forming ring in VII Zw466 (Appleton et al. 1996; Romano et al. 2008). An H I bridge connects VII Zw466 and G2 (Appleton et al. 1996). The scale bar at the bottom-right corner represents 10 kpc.

Table 1. General properties of VII Zw466 from Romano et al. (2008), Appleton et al. (1996) and de Vaucouleurs et al. (1991).

Property	
Right ascension (J2000)	12:32:04.4
Declination (J2000)	+66:24:16
Distance (D_L)	207 Mpc
Heliocentric velocity	14 490 km s^{-1}
Ring diameter	21.8 kpc
Stellar mass	4.83×10^{10} M$_\odot$
H I mass	4.1×10^9 M$_\odot$
SFR	7.8 M$_\odot$ yr^{-1}

fig. 2 of Appleton et al. 1996). Table 1 presents the general optical and H I properties of VII Zw466 (Appleton et al. 1996; Romano, Mayya & Vorobyov 2008).

Galaxy interactions can increase the density of H$_2$ molecular gas and lead to strong bursts of star formation (e.g. Henderson & Bekki 2016). However, previous CO observations have found collisional ring galaxies to be relatively deficient in molecular gas (e.g. Horellou et al. 1995). More recently, Higdon et al. (2011) have found evidence for enhancement in the rate of photodissociation of the molecular H$_2$ in these galaxies. That is, the destruction of ^{12}CO(1–0) appears to be more efficient relative to the molecular clouds within the star-forming discs of other field galaxies whose star formation is not triggered by the compression of the ISM (Higdon et al. 2011). Such extreme 'overcooked' ISM is likely to be dominated by small clouds and results in the underestimation of H$_2$ from ^{12}CO(1–0) observations when using the standard X_{CO} conversion (Higdon et al. 2011).

Typically, $N(H_2) = X_{CO} S_{CO}$ where $N(H_2)$ is the H$_2$ column density in units of cm^{-2} and S_{CO} is the integrated ^{12}CO(1–0) line intensity in K km s^{-1} (e.g. Bolatto, Wolfire & Leroy 2013). The alternative ^{12}CO(1–0)-to-H$_2$ conversion factor is α_{CO} where the molecular gas mass $M_{MOL} = \alpha_{CO} \times L_{CO}$ (Bolatto et al. 2013), where $L_{CO} = 2453 \, S_{CO} \Delta v D_L^2/(1+z)$ (Solomon & Vanden Bout 2005) in units of K km s^{-1} pc^2. The X_{CO} can be obtained by multiplying α_{CO} by 4.6×10^{19} (e.g. Sandstrom et al. 2013). The α_{CO} conversion factor includes a factor of 1.36 for helium.

Current theory suggests that high surface density regions (with greater gas temperatures and velocity dispersions) have a decreased X_{CO} value relative to that of our Galaxy (Narayanan et al. 2011, 2012). However, the accuracy of ^{12}CO(1–0) as a tracer of the total H$_2$ in low metallicity galaxies is more complex and difficult to determine. An increase in X_{CO} can be largely attributed to a contraction of the emitting surface area relative to that of the H$_2$ (Bolatto et al. 2013). In addition, this increase in X_{CO} may be further compounded or offset by a variation in brightness temperature due to variations in the heating sources (see section 6.1 of Bolatto et al. 2013 for a more detailed discussion). Therefore, despite recent advances in theoretical modelling (e.g. Narayanan et al. 2011, 2012; Shetty et al. 2011), the X_{CO} factor remains an area of significant uncertainty in the study of H$_2$ in collisional ring galaxies.

To further investigate the molecular gas properties in the potentially 'overcooked' ISM conditions of collisional ring galaxies, we search for ^{12}CO(1–0) in the ring galaxy VII Zw466. This galaxy is an excellent candidate for such an investigation because of the following: (1) we can discount the effects of metallicity, and (2) we have already assembled an excellent repository of multiwavelength observations such as the H I, H α and the far-infrared (FIR) to constrain the atomic gas and star formation properties of this galaxy.

A previous attempt to measure the molecular gas content of VII Zw466 has resulted only in upper limits (Appleton et al. 1999). The molecular component is the least-explored but one of the most crucial properties required to understand star formation. Therefore, the aims of this paper are as follows: (1) to determine the molecular gas content of VII Zw466 using the Large Millimeter Telescope Alfonso Serrano (LMT; Hughes et al. 2010), and (2) to determine the extent to which a variation of the X_{CO} value can affect our estimate of the total H$_2$ mass.

The details of our observations and processing can be found in Section 2. Section 3 presents the results of our observations. We discuss the implications of our results in Section 4 and Section 5 presents a summary of our findings. Throughout this paper, we adopt a ΛCDM cosmology of $\Omega_m = 0.27$, $\Omega_\Lambda = 0.73$, with a Hubble constant of $H_0 = 73$ km s^{-1} Mpc^{-1}.

2 OBSERVATIONS AND PROCESSING

2.1 Observations

The ^{12}CO(1–0) observations of VII Zw466 are obtained using the LMT (Hughes et al. 2010) and the Redshift Search Receiver (RSR; Erickson et al. 2007) that are being commissioned at the peak of Sierra Negra, Mexico. Our observations were obtained in 2015 June as part of the Early Science programme when only the inner 32 m of the 50-m primary reflector is fully operational. Upon completion, the LMT 50 m will become the world's largest dedicated millimeter single dish telescope, providing good spatial resolution and sensitivity to extended emission.
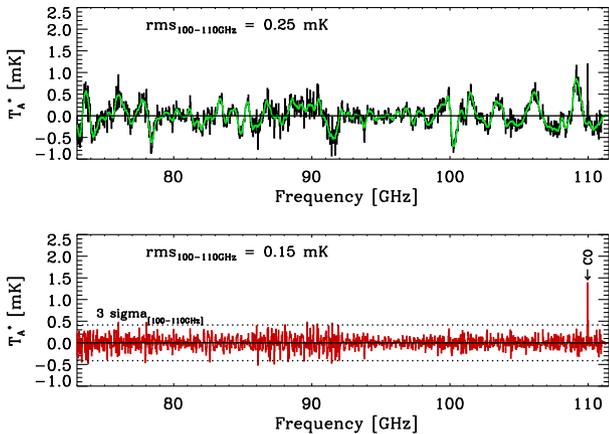
Figure 2. Fitting the calibrated RSR spectrum with a Savitzky–Golay (S–G) filter in order to account for the artefacts present in our bandpass. Top panel: the calibrated RSR spectrum overlaid with the fitted S–G filter (shown in green). Bottom panel: the final spectrum after the S–G filter has been subtracted. The dotted lines represent the $\pm 3\sigma$ level of this spectrum. The small arrows mark the location of the redshifted ^{12}CO(1–0) emission line. The brightness scale of the above spectra is that of T_A^*.

The RSR (Erickson et al. 2007; Chung et al. 2009; Snell et al. 2011) is the ideal instrument for the purposes of this project as it possesses an ultrawide bandwidth that spans the frequencies of 73–111 GHz with spectral channel widths of 31 MHz (corresponding to 100 km s^{-1} at 93 GHz). Such a wide bandwidth maximizes the number of molecular lines that can be observed in a single snapshot. The RSR beamsize ranges from 20 to 28 arcsec. We expect a beamsize of ~20 arcsec for the ^{12}CO(1–0) observations presented in this paper.

We observed VII Zw466 in a single pointing for a total integration time of 275 min over four nights (2015 June 7–19) in average weather conditions where $T_{sys} \sim 119$ K. Fig. 1 shows the location of this single pointing overlaid on the three-colour map of VII Zw466 from the Sloan Digital Sky Survey (SDSS; Alam et al. 2015).

The RSR has two beams that are used to observe the source and the sky simultaneously in order to account for the atmospheric contribution to our observations. Our observations were conducted using the 'wide beam throw' observing mode (where the two beams are separated by 294 arcsec). The telescope pointing calibrator, QSO 1153+495, was used.

2.2 Processing

Our observations are calibrated and processed using the latest version of DREAMPY, a software package written by G. Narayanan for the purposes of calibrating and reducing LMT-RSR observations. As the entire RSR 38-GHz bandwidth is distributed across six spectrometer boards, each individual spectrum is processed independently. A linear baseline is fitted and removed from each spectrum after the removal of bad channels and/or spectra containing strong baseline ripples. The resulting 38-GHz spectrum is produced by co-adding all the individual spectra with a $1/\sigma^2$ weighting. We show the reduced spectrum that has been corrected for atmospheric losses, rear spillover and scattering in Fig. 2 on the T_A^* scale.

Even though the RSR system and the DREAMPY reduction pipeline are optimized to improve the stability in the spectral baseline over the entire frequency range, some wide bandwidth artefacts remain (top panel of Fig. 2). To reduce the effects of the aperiodic ripples that remain in the reduced spectrum, we applied a Savitzky–Golay
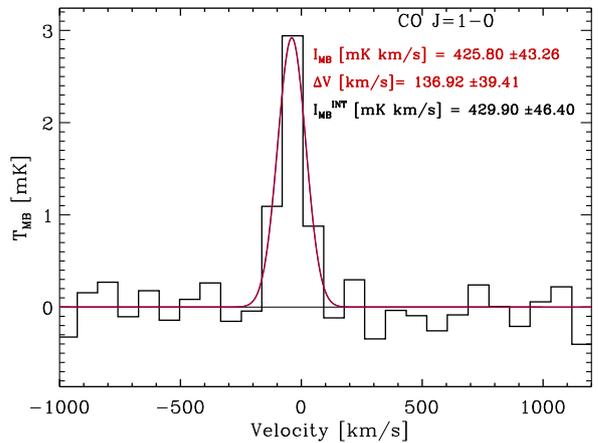

Figure 3. A Gaussian fit (red line) to the ^{12}CO(1–0) emission line from VII Zw466 on the T_{MB} scale. We assume the systemic velocity of VII Zw466 to be the heliocentric velocity (14 490 km s^{-1}) listed in Table 1.

(S–G) filter to the entire spectrum (Cybulski et al. 2016). We used an S–G filter with a second-order polynomial fitted with a width of 1 GHz. It should be noted that 1 GHz is significantly greater than the width of any expected molecular line in our spectrum. The bottom panel of Fig. 2 shows the resulting spectrum after the S–G filter has been applied. The rms of the spectrum between 100 and 111 GHz has decreased from 0.25 to 0.15 mK after the application of the S–G filter.

3 RESULTS

3.1 Integrated ^{12}CO(1–0) intensity

The redshifted ^{12}CO(1–0) emission line at 109.96 GHz is the only emission line found in our RSR observations of VII Zw466 (bottom panel of Fig. 2). To convert to the main beam temperature scale (T_{MB}), we estimate the efficiency factor to be 0.47 in the frequency range of 100–111 GHz. Fig. 3 presents our detection of this ^{12}CO(1–0) emission line (on the T_{MB} scale) with a signal-to-noise of ~10, centred on the assumed heliocentric velocity listed in Table 1. We fit the emission line profile with a Gaussian (represented by the red solid line in Fig. 3). We find the fitted velocity width to be 137 ($\pm$39) km s^{-1} and the fitted integrated flux to be 0.426 $\pm$ 0.043 K km s^{-1}. As the 31-MHz channel width corresponds to 84.5 km s^{-1} at 109.96 GHz, we find the ^{12}CO(1–0) line width to be 108 ($\pm$50) km s^{-1}. Uncertainties for the fitted parameters are obtained via bootstrap resampling.

For comparison, the integrated flux (S_{CO}) measured from the reduced spectrum is 0.430 $\pm$ 0.046 K km s^{-1}. Following Solomon & Vanden Bout (2005), we estimate the CO luminosity (L_{CO}) of VII Zw466 to total 1.6 ($\pm$0.5) $\times$ 10^8 K km s^{-1} pc^2. Assuming a uniform distribution of ^{12}CO(1–0) across the entire galaxy, we estimate a total S_{CO} of 1.229 $\pm$ 0.078 K km s^{-1} for VII Zw466 since our single 20-arcsec pointing covers only 35 per cent of VII Zw466. Therefore, we deduce that the total L_{CO} of the entire ring galaxy to be 4.6 ($\pm$0.8) $\times$ 10^8 K km s^{-1} pc^2.

Using the correlations for weakly and strongly interacting galaxies from Solomon & Sage (1988), we estimate L_{CO} from the FIR luminosity (L_{FIR}; from the *IRAS* Faint Source Catalog Moshir et al. 1990) to range from 1.55 $\times$ 10^{10} to 1.49 $\times$ 10^9 K km s^{-1} pc^2 for weakly and strongly interacting galaxies, respectively. Assuming that collisional ring galaxies such as VII Zw466 can be classified

as a strongly interacting star-forming galaxy, the estimated total L_{CO} is approximately 30.9 per cent of the expected L_{CO}. Therefore, our measured L_{FIR}/L_{CO} fraction is greater than that measured in giant molecular clouds (GMC) in the Galaxy (Solomon et al. 1987; Mooney & Solomon 1988). On the other hand, the L_{FIR}/L_{CO} fraction found for VII Zw466 is comparable to 11 of the 14 merging galaxies examined by Solomon & Sage (1988).

3.2 H_2 molecular gas in VII Zw466

The H_2 content of a galaxy provides one of the fundamental building blocks from which stars form. Since cold H_2 is not directly observable, astronomers typically infer the H_2 content of galaxies from observations of $^{12}CO(1–0)$. Many studies have found the X_{CO} conversion factor to vary depending on galactic environment, interaction history and metallicities (e.g. Scoville et al. 1991; Wilson 1995; Solomon et al. 1997; Hinz & Rieke 2006; Bolatto et al. 2008; Meier et al. 2010; Leroy et al. 2011; Genzel et al. 2012).

Recently, detailed theoretical simulations by Narayanan et al. (2012) have modelled the X_{CO} conversion factors as a function of the metallicity and CO line intensity. As the metallicity of VII Zw466 is approximately solar ($Z = 1$; Bransford et al. 1998), the metallicity term in equation (10) of Narayanan et al. (2012) equals 1.0 and equation (10) can be rewritten as

$$X_{CO} = \min[4, 6.75 \times \langle S_{CO} \rangle^{-0.32}] \times 10^{20} \ \text{cm}^{-2}(\text{K km s}^{-1})^{-1}, \tag{1}$$

where S_{CO} is the integrated $^{12}CO(1–0)$ brightness on the T_{MB} scale in units of K km s^{-1}. The minimum value is adopted for X_{CO} from the above equation because at low values of S_{CO}, X_{CO} appears to be independent of the galactic environment and is limited mainly by the fixed galaxy properties (see Narayanan et al. 2012 for more details). Using equation (1) above, we find X_{CO} to be approximately 3.74×10^{20} cm^{-2} (K km s^{-1})$^{-1}$.

Using $M_{H2} = 5.5 X_{CO}(2 \times 10^{20})^{-1} L_{CO}$ K km s^{-1} pc^2 (Leroy et al. 2009) and assuming $X_{CO} = 3.74 \times 10^{20}$, we find the H_2 mass of VII Zw466 to be 4.7×10^9 M$_\odot$. We note that this model-derived X_{CO} is approximately 1.9 times the solar neighbourhood value of $X_{CO} = 2 \times 10^{20}$ cm^{-2} (K km s^{-1})$^{-1}$ (Solomon et al. 1987; Strong & Mattox 1996; Dame, Hartmann & Thaddeus 2001). Consequently, the estimated H_2 mass is also greater by a factor of 1.9.

To ascertain the reliability of our derived H_2 mass, we test a second prescription for the $^{12}CO(1–0)$-to-H_2 conversion factor. Bolatto et al. (2013) recommend a simple determination for the conversion based upon the metallicity (Z'), the average surface density of molecular clouds (Σ_{GMC} in units of 100 M$_\odot$ pc^{-2}) and the total stellar plus gas density (Σ_{TOT}):

$$\alpha_{CO} \approx 2.9 \exp\left(\frac{+0.4}{Z'\Sigma_{GMC}}\right)\left(\frac{\Sigma_{TOT}}{100\,\text{M}_\odot\,\text{pc}^{-2}}\right)^{-\gamma}, \tag{2}$$

where α_{CO} is in units of M$_\odot$ (K km s^{-1} pc^2)$^{-1}$, and $\gamma \approx 0.5$ for $\Sigma_{TOT} > 100$ M$_\odot$ pc^{-2} (Bolatto et al. 2013).

Approximating the lower limit of the total stellar plus gas density to be the total stellar plus H I gas density, we assume that all the gas and stars are located within the ring of VII Zw466 – a torus with inner and outer diameters of 11 and 21.8 kpc, respectively (Appleton & Struck-Marcell 1987; Romano et al. 2008). We estimate a total surface area of 278.2 kpc^2. This is clearly a rough approximation; however, it suffices for the purpose of approximating the minimum total density of the ring. As such, we find $\Sigma_{TOT} \gtrsim 188$ M$_\odot$ pc^{-2} for the ring of VII Zw466.

Estimating Σ_{GMC} is difficult. While we expect high GMC densities due to the confinement of the majority of the VII Zw466 ISM to be within the star-forming ring, the consequence of such ISM confinement actually leads to the enhanced destruction of molecular clouds due to (1) expanding H II regions (Bally & Scoville 1980; Maddalena & Morris 1987); and (2) cloud–cloud collisions (Appleton & Struck-Marcell 1987). This results in smaller molecular cloud fragments and photodissociated H I (e.g. Higdon et al. 2011). If we assume a fiducial minimum and maximum Σ_{GMC} of 40 and 188 M$_\odot$ pc^{-2}, we find that the Bolatto et al. (2013) prescription results in α_{CO} of 5.7 and 3.3 M$_\odot$ (K km s^{-1} pc^2)$^{-1}$, respectively. These α_{CO} values correspond to X_{CO} of 2.6×10^{20} and 1.5×10^{20} cm^{-2} (K km s^{-1})$^{-1}$. Therefore, the estimated H_2 mass for VII Zw466 ranges from 1.9×10^9 to 3.3×10^9 M$_\odot$ using the prescription from Bolatto et al. (2013) in combination with the assumption that Σ_{GMC} ranges between 40 and 188 M$_\odot$ pc^{-2}.

For a standard Milky Way $\alpha_{CO} = 4.4$ M$_\odot$ (K km s^{-1} pc^2)$^{-1}$ (e.g. Strong & Mattox 1996; Dame et al. 2001), we estimate M_{H2} to be 2.6×10^9 M$_\odot$. Do the extreme ISM conditions within the ring of this collisional galaxy lead to a variation of the X_{CO} value as a result of reduced shielding of molecular clouds against feedback effects (Higdon et al. 2011, 2015) ? We find from our estimations above that such variations in X_{CO} values are likely to be relatively small and may only be factors of 0.8–1.9 different to the standard Galactic value. As such, we estimate that the M_{H2} of VII Zw466 to be between 1.9×10^9 and 4.7×10^9 M$_\odot$.

4 DISCUSSION

4.1 Comparing our estimated M_{H2} to previous studies and known scaling relations

In this section, we demonstrate the extreme ISM and star formation properties of collisional ring galaxies by comparing multiwavelength observations of VII Zw466 to standard scaling relationships and correlations found in samples of nearby star-forming galaxies.

A previous search for H_2 in VII Zw466 yielded an upper limit of $<1.2 \times 10^9$ M$_\odot$ [using $X_{CO} = 2.3 \times 10^{20}$ cm^{-2} (K km s^{-1})$^{-1}$; Appleton et al. 1999]. When we adopt the same X_{CO} value as Appleton et al. (1999), we find a total M_{H2} of 2.9×10^9 M$_\odot$. Such a discrepancy in total M_{H2} between the two sets of observations argues strongly against our previous assumption that the H_2 content is uniformly distributed across this galaxy. As such, it is likely that the observed M_{H2} in our single LMT pointing accounts for at least 84 per cent of the total M_{H2} in VII Zw466.

Using the 60 and 100-μm observations from the *IRAS* Faint Source Catalog (Moshir et al. 1990), we estimate that the L_{FIR} of VII Zw466 is 2.73×10^{10} L$_\odot$. From L_{FIR}, we would expect L_{CO} to be 8.4×10^8 and 1.6×10^8 K km s^{-1} pc^2 from the isolated and strongly interacting L_{FIR}–L_{CO} correlations of Solomon & Sage (1988). Therefore, if we classify VII Zw466 as a strongly interacting galaxy, we appear to have observed the total L_{CO} that can be expected from the L_{FIR} of VII Zw466.

Analogous to the L_{FIR}–L_{CO} correlation, the L_{CO}–SFR correlation is often observed in samples of low-redshift star-forming galaxies (e.g. Saintonge et al. 2012). However, the L_{CO}–SFR correlation is likely to be stronger, since we know that $^{12}CO(1–0)$ exists within the molecular clouds from which stars form, whereas the L_{FIR}–L_{CO} correlation is correlating the emission from the younger stellar population with the molecular gas content. We find that the L_{CO} and SFR for VII Zw466 is consistent with the observed L_{CO}–SFR correlation from Saintonge et al. (2012). In particular, our observed

L_{CO} from the LMT single pointing and the SFR within the region (assuming SFR = 2.7 $M_\odot$ yr^{-1}) is consistent with gas depletion times between a few hundred Myr to 1 Gyr. In this case, the inferred depletion times vary depending on the assumed X_{CO}. However, the main result here is that the L_{CO} and SFR of VII Zw466 are consistent with star-forming galaxies at low redshifts (Saintonge et al. 2012) and the general Kennicutt–Schmidt relationship.

If we assume the H_2 star formation efficiency (ratio of SFR to M_{H2}) to be a constant (as is often assumed for nearby star-forming galaxies; e.g. Leroy et al. 2008; Wong et al. 2016), we can estimate the H_2 surface density from the star formation rate density via this expression:

$$\Sigma_{H2} \approx \frac{10^{-6}\Sigma_{SFR}}{9.51 \times 10^{-10}} \ M_\odot \ pc^{-2}, \tag{3}$$

where the star formation rate surface density (Σ_{SFR}) is in units of $M_\odot$ yr^{-1} kpc^{-2} (Leroy et al. 2008; Zheng et al. 2013; Wong et al. 2016). Using the observed SFR from Romano et al. (2008), we find that VII Zw466 has an estimated $\Sigma_{SFR} = 2.8 \times 10^{-2}$ $M_\odot$ yr^{-1} kpc^{-2} and $\Sigma_{H2} = 29.4$ $M_\odot$ pc^{-2}. Within the region observed by the LMT single pointing (35 per cent of the total surface area estimated in Section 3.2), we expect $M_{H2} = 2.9 \times 10^9$ $M_\odot$, a factor of at least 1.8 greater than that estimated from our early science LMT ^{12}CO(1–0) observations assuming a non-Galactic X_{CO} conversion factor. Such a result suggests that the star formation efficiency of VII Zw466 may not be consistent with those of other nearby star-forming galaxies.

More recently, Huang & Kauffmann (2014) found that the global molecular gas depletion time ($t_{dep} = \frac{M_{H2}}{SFR}$) correlates strongly with the specific star formation rate (sSFR = $\frac{SFR}{M_{stellar}}$). Using the total stellar mass and global star formation rate of VII Zw466 from Table 1, we find log sSFR = −9.8 yr^{-1}. Following the sSFR–t_{dep} correlation from Huang & Kauffmann (2014) for a sample of nearby galaxies from the HERA CO-Line Extragalactic Survey (HERACLES) survey (Leroy et al. 2009), we expect log t_{dep} = 9.2. If VII Zw466 is a star-forming galaxy that is comparable to the HERACLES survey of nearby star-forming galaxies, we would expect VII Zw466 to have $M_{H2} = 1.2 \times 10^{10}$ $M_\odot$ given its observed star formation rate and stellar mass from Romano et al. (2008). In our case of VII Zw466, the sSFR–t_{dep} correlation predicts M_{H2} to be a factor of 3–6 greater than the total M_{H2} estimated from our ^{12}CO(1–0) observations. In order to derive such a high M_{H2} from our ^{12}CO(1–0) observations, we would require $X_{CO} = 9.5 \times 10^{20}$ as well as $\Sigma_{GMC} = 17.6$ $M_\odot$ pc^{-2} using the prescription from Bolatto et al. (2013). Such an extreme X_{CO} suggest that it is unlikely that any apparent H_2 deficiency of VII Zw466 is due simply to the assumed X_{CO}. Therefore, any apparent H_2 deficiency may either be real or that VII Zw466 is dominated by CO-dark gas and as such, is only ^{12}CO(1–0)-deficient. See Section 4.3 for further discussions on CO-dark gas.

We hypothesize that a CO-deficient result is a more extreme form of the '[C II]–FIR deficit' found in ultraluminous infrared galaxies (ULIRGs) at $z = 0$ where only approximately 10 per cent of the expected [C II] luminosity is observed (e.g. Malhotra et al. 1997, 2001; Graciá-Carpio et al. 2011; Narayanan & Krumholz 2016). The [C II] emission originates from the outer layers of molecular clouds that are destroyed by the strong starbursts in ULIRGs. While CO resides in more shielded regions of molecular clouds than [C II] (Narayanan & Krumholz 2016), we posit that there is insufficient shielding of the CO molecules from destruction by *in situ* star formation feedback due to the strong confinement of the galaxy's ISM in the ring.

4.2 Atomic hydrogen and the molecular-to-atomic hydrogen ratio

Atomic hydrogen (H I) can provide the initial gas reservoir from which molecular clouds form, as well as the by-product of H_2 photodissociation (e.g. Allen, Heaton & Kaufman 2004; Higdon, Higdon & Rand 2011). The H I-normalized star formation efficiency (SFE$_{H I}$ = SFR/$M_{H I}$) is surprisingly uniform for nearby star-forming galaxies spanning across five orders of magnitude in stellar masses (e.g. Wong et al. 2016). However, we find that VII Zw466 has an SFE$_{H I}$ = $10^{-8.72}$ yr^{-1}. This SFE$_{HI}$ is greater by factors of 6–17 relative to both the average SFE$_{H I}$ found in stellar-mass selected and H I-mass selected samples of star-forming galaxies (Schiminovich et al. 2010; Huang et al. 2012; Wong et al. 2016). Hence, the enhanced star formation rate and the possible H I deficiency of this collisional ring galaxy make it an extreme outlier in terms of ISM and star formation properties relative to other noninteracting star-forming galaxies.

Even though some studies find that stars do not form solely from H_2 but from cool gas ($T < 100$ K) that are able to shield itself from the interstellar radiation field (ISRF; e.g. Glover & Clark 2012; Hu et al. 2016), it is commonly thought that stars form from H_2 (e.g. Leroy et al. 2008). Assuming that the majority of stars form from H_2, the ratio of molecular-to-atomic hydrogen (R_{mol}) reflects the efficiency with which molecular clouds form. The R_{mol} of nearby galaxies have been found to strongly depend on local conditions since the H I is more susceptible than the H_2 to tidal and ram pressure stripping (e.g. Chung et al. 2007; Vollmer et al. 2012). Processes such as tidal and ram pressure stripping are able to remove a significant amount of H I from galaxies. Indeed, previous H I observations of VII Zw466 by Appleton et al. (1996) reveal a disturbed H I morphology that bridges both VII Zw466 and its neighbour, G2, as a result of past tidal interactions between these two galaxies. Such displacement of the H I reservoir is likely to contribute to the H I deficiency of VII Zw466. On the other hand, recent studies have found that the R_{mol} in disc galaxies are generally governed by the hydrostatic disc pressure (Elmegreen 1989; Wong et al. 2016), and easily traced by the stellar surface density (Σ_*; Leroy et al. 2008; Wong et al. 2013). In addition to the disc pressure and the stellar potential, stellar feedback may also play a critical role in gas collapse and molecular cloud formation (Elmegreen 1993; Elmegreen & Parravano 1994; Hunter, Elmegreen & Baker 1998; Wong & Blitz 2002; Blitz & Rosolowsky 2004, 2006).

The transition between an H I-dominated ISM and an H_2-dominated ISM occurs when $\Sigma_* = 81$ $M_\odot$ pc^{-2}, $R_{mol} = \Sigma_*/81$ $M_\odot$ pc^{-2} (Leroy et al. 2008). We estimate Σ_* to be 173 $M_\odot$ pc^{-2}, placing VII Zw466 in the H_2-dominated ISM regime. Similar to other H I-rich collisional ring galaxies (e.g. Higdon et al. 2011, 2015; Parker et al. 2015), VII Zw466 resides in a significant reservoir of H I (Appleton et al. 1996). In fact, the expected R_{mol} from the estimated Σ_* is 1.4. This translates to an expected $M_{H2} = 5.6 \times 10^9$ $M_\odot$, assuming the observed H I mass of 4.1×10^9 $M_\odot$ (see Table 1; Appleton et al. 1996).

Assuming a uniform distribution of H_2 across the entire galaxy, we estimate the total M_{H2} from our ^{12}CO(1–0) observations to range between 1.9×10^9 and 4.7×10^9 $M_\odot$ (see Section 3.2). However, if this assumption is incorrect (as discussed in Section 4.1) and our LMT observations have detected the majority if not all the available ^{12}CO(1–0) in VII Zw466, then the expected M_{H2} from the estimated Σ_* is likely to be a factor of 5 greater than both our single pointing observations and those of Appleton et al. (1999).

Unless a significant amount of CO in VII Zw466 is in the form of CO-dark gas, the estimated R_{mol} from our LMT observations in combination with those of Appleton et al. (1999) range from 0.18 to 0.29 depending on the assumed CO-to-H_2 conversion factor. Therefore it appears that the molecular gas content of collisional ring galaxies such as VII Zw466 are possibly deficient relative to its atomic gas content, which may also be deficient. This result is consistent with the idea of enhanced destruction of molecular clouds through star formation feedback within the confined ring ISM.

4.3 CO-dark molecular gas

So far, we have not included the contribution of CO-dark molecular gas into our estimation of H_2 in VII Zw466. Therefore it is possible that we have underestimated the molecular gas reservoir in VII Zw466. To recover the expected amount of M_{H2} from known scaling relationships, the amount of dark CO gas will have to be at least 2.6 times that of the CO-bright gas.

Recent high-resolution hydrodynamic simulations of the ISM in a Milky Way analogue have found $^{12}CO(1–0)$-dark gas to exist in a diffused, low surface density state that is typically less shielded from the ISRF (Smith et al. 2014; Glover & Smith 2016). A galaxy–galaxy collision is the physical mechanism by which the high-density ring of VII Zw466 formed. However, we do not have sufficient angular resolution in the gas mapping [$^{12}CO(1–0)$ and H I] of this system to accurately determine the gas densities. Therefore, we are unable to rule out the possibility for CO-dark gas in collisional ring galaxies even though the confined high surface density ISM within the ring is in theory not ideal for the existence of dark CO gas. While it is currently beyond the scope of this paper to provide further constraints on the amount of dark CO gas, future observations of the millimetre dust continuum (e.g. Wall et al. 2016), higher order CO transition lines, other ionized carbon lines such as [C II] (e.g. Herrera-Camus et al. 2015; de Blok et al. 2016) and high-density tracers such as HCN or HNC can be used to help constrain the gas densities and possibly the existence of CO-dark gas in VII Zw466.

4.4 Implications

Many models (e.g. Narayanan & Krumholz 2016) make the assumption that R_{mol} increases as surface density of molecular clouds increases. In general, this is confirmed by observations of both interacting and non-interacting star-forming galaxies in the nearby Universe. However, our $^{12}CO(1–0)$ observations and those of Horellou et al. (1995) and Appleton et al. (1999) find that the molecular gas content of collisional ring galaxies may not be consistent with this assumption. The main reason for this is because the entire star-forming ISM of the galaxy is now confined to within the ring that is formed by the expanding density wave after the collision. While we expect a temporary increase in the H_2 fraction shortly after the collision (due to compression of the ISM), the amount of H_2 is likely to decline quickly following its consumption via the strong bursts of star formation within the ring in the first 10 Myr (e.g. Pellerin et al. 2010; Henderson & Bekki 2016). Alternatively, the high H_2 fractions of collisional ring galaxies such as VII Zw466 may remain hidden due to a CO deficiency. We think that a CO deficiency is less likely since our observations of VII Zw466 are consistent with the general Kennicutt–Schmidt and the L_{CO}–SFR correlations that are typically found from star-forming galaxies.

The stellar and ISM properties of interacting galaxies are still typically dominated by standard ISM conditions in regions that are unaffected or shielded from the effects of the interactions, in addition to the interaction-affected regions. These interactions (be they tidal or ram pressure) are typically not strong enough to alter the density of both the stellar component and the ISM of the entire galaxy.

Therefore, collisional galaxies represent a galactic-wide accelerated mode of star formation evolution whereupon the first episode of interaction-triggered starburst immediately has a negative impact upon the potential for subsequent star formation episodes. This argument is supported by young stellar ages observed in the stellar population of the ring in collisional ring galaxies (Pellerin et al. 2010). Such extreme modes of star formation histories may be more important at high redshifts when collisions are likely to be more common. As such, the understanding of star formation under extreme conditions is likely to impact our theoretical understanding of gas, star formation and feedback throughout the cosmic history of the Universe.

5 SUMMARY AND CONCLUSIONS

We report the discovery of $^{12}CO(1–0)$ in the ring galaxy VII Zw466 using the RSR instrument during the early science commissioning phase of the LMT. We find the CO luminosity (L_{CO}) of VII Zw466 to be 1.6×10^8 K km s^{-1} pc^2.

Recent studies have found that $^{12}CO(1–0)$ observations of collisional ring galaxies are likely to underestimate the true amount of H_2 using the standard Galactic X_{CO} value. In this paper, we test two different prescriptions for converting between the observed $^{12}CO(1–0)$ emission to the inferred M_{H2} from Narayanan et al. (2012) and Bolatto et al. (2013). Using these two prescriptions, we find that the estimated H_2 mass for VII Zw466 is a factor of 0.9–1.9 times greater than that found from the standard solar neighbourhood X_{CO} value. The estimated M_{H2} for VII Zw466 from our LMT observations ranges between 7.5×10^8 and 1.6×10^9 M$_\odot$.

If we assume a uniform H_2 distribution and scale the observed M_{H2} to account for the entire surface area of VII Zw466, our estimated total M_{H2} ranges between 1.9×10^9 and 4.7×10^9 M$_\odot$. However, we think that such an assumption may not be valid since previous observations by Appleton et al. (1999) have found an M_{H2} upper limit of $<1.2 \times 10^9$ M$_\odot$ for this galaxy. Therefore, we posit that our LMT $^{12}CO(1–0)$ observations have detected the majority of the $^{12}CO(1–0)$ content in this galaxy and that the molecular gas is not likely to be evenly distributed across the entire galaxy.

We conclude that collisional ring galaxies represent the extreme end of galaxy interactions and evolution whereby the ISM and star-forming properties are distinct from other star-forming galaxies that are isolated or experiencing non-collisional interactions. Our results suggest that the H_2 deficiency in the star-forming environment of the ring is likely real unless there exists a significant amount of CO-dark gas. Also the apparent H_2 deficiency is unlikely to be explained by the variation of X_{CO} from the standard Galactic value.

REFERENCES

Alam S. et al., 2015, ApJS, 219, 12

Allen R. J., Heaton H. I., Kaufman M. J., 2004, ApJ, 608, 314

Appleton P. N., Marston A. P., 1997, AJ, 113, 201

Appleton P. N., Struck-Marcell C., 1987, ApJ, 312, 566

Appleton P. N., Charmandaris V., Struck C., 1996, ApJ, 468, 532

Appleton P. N., Charmandaris V., Horellou C., Mirabel I. F., Ghigo F., Higdon J. L., Lord S., 1999, ApJ, 527, 143

Bally J., Scoville N. Z., 1980, ApJ, 239, 121

Blitz L., Rosolowsky E., 2004, ApJ, 612, L29

Blitz L., Rosolowsky E., 2006, ApJ, 650, 933

Bolatto A. D., Leroy A. K., Rosolowsky E., Walter F., Blitz L., 2008, ApJ, 686, 948

Bolatto A. D., Wolfire M., Leroy A. K., 2013, ARA&A, 51, 207

Bransford M. A., Appleton P. N., Marston A. P., Charmandaris V., 1998, AJ, 116, 2757

Chung A., van Gorkom J. H., Kenney J. D. P., Vollmer B., 2007, ApJ, 659, L115

Chung A., Narayanan G., Yun M. S., Heyer M., Erickson N. R., 2009, AJ, 138, 858

Cybulski R. et al., 2016, MNRAS, 459, 3287

Dame T. M., Hartmann D., Thaddeus P., 2001, ApJ, 547, 792

de Blok W. J. G. et al., 2016, AJ, 152, 51

de Vaucouleurs G., de Vaucouleurs A., Corwin H. G., Jr, Buta R. J., Paturel G., Fouqué P., 1991, Third Reference Catalogue of Bright Galaxies. Volume I: Explanations and References. Volume II: Data for Galaxies between 0^h and 12^h. Volume III: Data for Galaxies between 12^h and 24^h. Springer-Verlag, New York

Elmegreen B. G., 1989, ApJ, 338, 178

Elmegreen B. G., 1993, ApJ, 411, 170

Elmegreen B. G., Parravano A., 1994, ApJ, 435, L121

Erickson N., Narayanan G., Goeller R., Grosslein R., 2007, in Baker A. J., Glenn J., Harris A. I., Mangum J. G., Yun M. S., eds, ASP Conf. Ser. Vol. 375, From Z-Machines to ALMA: (Sub)Millimeter Spectroscopy of Galaxies. Astron. Soc. Pac., San Francisco, p. 71

Fiacconi D., Mapelli M., Ripamonti E., Colpi M., 2012, MNRAS, 425, 2255

Genzel R. et al., 2012, ApJ, 746, 69

Glover S. C. O., Clark P. C., 2012, MNRAS, 421, 9

Glover S. C. O., Smith R. J., 2016, MNRAS, 462, 3011

Graciá-Carpio J. et al., 2011, ApJ, 728, L7

Henderson B., Bekki K., 2016, ApJ, 822, L33

Herrera-Camus R. et al., 2015, ApJ, 800, 1

Higdon J. L., Higdon S. J. U., Rand R. J., 2011, ApJ, 739, 97

Higdon J. L., Higdon S. J. U., Martín Ruiz S., Rand R. J., 2015, ApJ, 814, L1

Hinz J. L., Rieke G. H., 2006, ApJ, 646, 872

Horellou C., Casoli F., Combes F., Dupraz C., 1995, A&A, 298, 743

Hu C.-Y., Naab T., Walch S., Glover S. C. O., Clark P. C., 2016, MNRAS, 458, 3528

Huang M.-L., Kauffmann G., 2014, MNRAS, 443, 1329

Huang S., Haynes M. P., Giovanelli R., Brinchmann J., 2012, ApJ, 756, 113

Hughes D. H. et al., 2010, in Stepp L. M., Gilmozzi R., Hall H. J., eds, Proc. SPIE Conf. Ser. Vol. 7733, Ground-based and Airborne Telescopes III. SPIE, Bellingham, p. 12

Hunter D. A., Elmegreen B. G., Baker A. L., 1998, ApJ, 493, 595

Leroy A. K., Walter F., Brinks E., Bigiel F., de Blok W. J. G., Madore B., Thornley M. D., 2008, AJ, 136, 2782

Leroy A. K. et al., 2009, AJ, 137, 4670

Leroy A. K. et al., 2011, ApJ, 737, 12

Lynds R., Toomre A., 1976, ApJ, 209, 382

Maddalena R. J., Morris M., 1987, ApJ, 323, 179

Malhotra S. et al., 1997, ApJ, 491, L27

Malhotra S. et al., 2001, ApJ, 561, 766

Mapelli M., Mayer L., 2012, MNRAS, 420, 1158

Meier D. S., Turner J. L., Beck S. C., Gorjian V., Tsai C.-W., Van Dyk S. D., 2010, AJ, 140, 1294

Mooney T. J., Solomon P. M., 1988, ApJ, 334, L51

Moshir M. et al., 1990, in IRAS Faint Source Catalogue, version 2.0

Narayanan D., Krumholz M., 2016, MNRAS, preprint (arXiv:1601.05803)

Narayanan D., Krumholz M., Ostriker E. C., Hernquist L., 2011, MNRAS, 418, 664

Narayanan D., Krumholz M. R., Ostriker E. C., Hernquist L., 2012, MNRAS, 421, 3127

Parker Q. A., Zijlstra A. A., Stupar M., Cluver M., Frew D. J., Bendo G., Bojičić I., 2015, MNRAS, 452, 3759

Pellerin A., Meurer G. R., Bekki K., Elmegreen D. M., Wong O. I., Knezek P. M., 2010, AJ, 139, 1369

Romano R., Mayya Y. D., Vorobyov E. I., 2008, AJ, 136, 1259

Saintonge A. et al., 2012, ApJ, 758, 73

Sandstrom K. M. et al., 2013, ApJ, 777, 5

Schiminovich D. et al., 2010, MNRAS, 408, 919

Scoville N. Z., Sargent A. I., Sanders D. B., Soifer B. T., 1991, ApJ, 366, L5

Shetty R., Glover S. C., Dullemond C. P., Ostriker E. C., Harris A. I., Klessen R. S., 2011, MNRAS, 415, 3253

Smith R. J., Glover S. C. O., Clark P. C., Klessen R. S., Springel V., 2014, MNRAS, 441, 1628

Snell R. L., Narayanan G., Yun M. S., Heyer M., Chung A., Irvine W. M., Erickson N. R., Liu G., 2011, AJ, 141, 38

Solomon P. M., Sage L. J., 1988, ApJ, 334, 613

Solomon P. M., Vanden Bout P. A., 2005, ARA&A, 43, 677

Solomon P. M., Rivolo A. R., Barrett J., Yahil A., 1987, ApJ, 319, 730

Solomon P. M., Downes D., Radford S. J. E., Barrett J. W., 1997, ApJ, 478, 144

Strong A. W., Mattox J. R., 1996, A&A, 308, L21

Vollmer B., Wong O. I., Braine J., Chung A., Kenney J. D. P., 2012, A&A, 543, A33

Wall W. F. et al., 2016, MNRAS, 459, 1440

Wilson C. D., 1995, ApJ, 448, L97

Wong T., Blitz L., 2002, ApJ, 569, 157

Wong O. I. et al., 2006, MNRAS, 370, 1607

Wong T. et al., 2013, ApJ, 777, L4

Wong O. I., Meurer G. R., Zheng Z., Heckman T. M., Thilker D. A., Zwaan M. A., 2016, MNRAS, 460, 1106

Zheng Z., Meurer G. R., Heckman T. M., Thilker D. A., Zwaan M. A., 2013, MNRAS, 434, 3389

This paper has been typeset from a TeX/LaTeX file prepared by the author.